ACS OMEGA

Open Access



http://pubs.acs.org/journal/acsodf

Article

# Comprehensive Study on Mineral Processing Methods and Mineral Technical Economics of Manganese Ore in Chongqing Chengkou

Wensheng Li, Guangchao Jiang, Guangzhou Yang, and Facheng Qiu*

Cite This: *ACS Omega* 2024, 9, 10929−10936

Read Online



**ABSTRACT:** Chongqing Chengkou manganese deposit is a large carbonate-type manganese deposit in the upper reaches of the Yangtze River, located in Gaoyan Town, Chengkou County, Chongqing. In order to improve the recovery rate of low-grade manganese ore and concentrate grade index, achieve efficient utilization of mineral resources, and sustainable development of Gaoyan manganese ore deposit in Chengkou, Chongqing, China, in this paper, by means of optical microscope analysis, high-resolution X-ray tomography technology, three-dimensional image analysis technology, X-ray diffraction analysis, X-ray fluorescence spectrum analysis, and technical and economic analysis, the occurrence state and process mineralogy of manganese are studied, and the technical and economic analysis of flotation, high-intensity magnetic separation, and gravity separation are carried out. It provides a reference for other mining enterprises to choose the most suitable beneficiation method according to the specific mineral species.

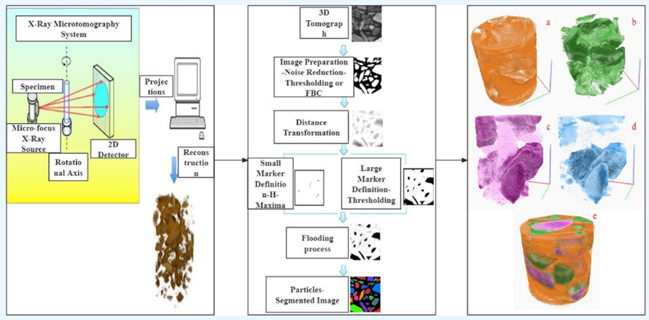


## 1. INTRODUCTION

Manganese ore is an important strategic mineral resource.[1] China is the world's main producer and consumer of manganese ore, with reserves of about 570 million tons, accounting for about 34% of the world's total reserves. Manganese ore is mainly used in the production of steel, alloys, batteries, and chemical products. In modern industry, manganese and its compounds are used in various fields. Among them, the most important use of manganese is the metallurgical industry; the amount of manganese reached more than 90%, mainly used in the smelting process of steel, as a Deoxidizer and desulfurizer. The remaining 10% or so of manganese is used in other industrial fields, such as the chemical industry for the manufacture of various manganese salts, light industry for batteries, printing coatings, etc., building materials industry for glass colorants and fading agents, as well as the defense industry and environmental protection industry have also been applied. The Chengkou manganese deposit in Chongqing is a large carbonate-type manganese deposit in the upper reaches of the Yangtze River in China, which is mainly composed of the Gaoyan manganese deposit (West mining area) in the west of Chengkou County in Chongqing and the Daduxi Manganese deposit (East Mining area) in the southeast of Chengkou County in Chongqing. The Chengkou manganese ore in Chongqing is mainly low-grade manganese ore with a complex mineral composition, which is a typical high-phosphorus poor manganese ore. The genetic types of manganese ore mainly include sedimentary type and weathering type; sedimentary type is the main type of manganese ore. The weathered manganese ore occurs locally on the surface, and the mineral resources are relatively small, so it cannot form a concentrated scale. However, the Chengkou manganese ore deposit in Chongqing is a sedimentary carbonate manganese deposit with relatively concentrated distribution, so its manganese ore resources are rich, but due to its complex mineral composition, the resource utilization rate is low.

At present, the domestic and foreign research on the ore process mineralogy is mainly through chemical phase analysis, X-ray diffraction analysis, chemical multielement analysis, scanning electron microscopy, electron probe, and other methods to complete; thus, to determine the mineral composition, chemical composition, mineral particle size characteristics, and distribution law, the study of manganese ore is almost the same. The influence of mineralogical factors on the recovery of manganese was analyzed from the perspective of process mineralogy to determine the mineral processing method and process flow. In 1998, Min Jianping

Received: December 22, 2023
Revised: February 13, 2024
Accepted: February 14, 2024
Published: February 26, 2024

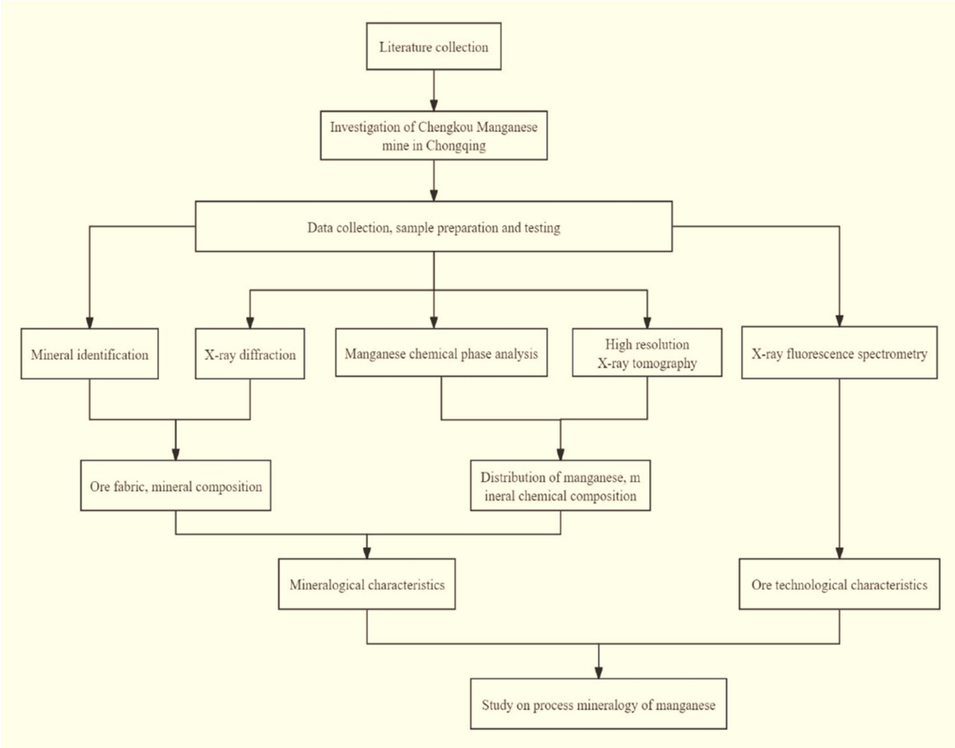


**Figure 1.** Technical roadmap for process mineralogy of manganese.

studied process mineralogy by collecting carbonate-type manganese ore from Chengkou of Chongqing and proposed that phosphorus in manganese ore of Chengkou of Chongqing is mainly distributed in the form of collophosphates. Then, the dephosphorization experiments were carried out by two kinds of dephosphorization processes, respectively, and it was proved that the dephosphorization efficiency of the high-intensity magnetic separation process was obviously better than that of the heavy separation process. The use of process mineralogy in combination with investment evaluation methods based on net present value (NPV), payback period (PBP), and internal rate of return (IRR) has significant advantages in mining investment decisions: (1) Enhanced decision accuracy: Process mineralogy focuses on the physical and chemical properties of ores, which are critical in determining the most efficient processing methods. Understanding these characteristics can help investors more accurately estimate the potential costs and benefits of a project, which in turn improves the accuracy of decision-making when using financial metrics such as NPV and IRR for evaluation. (2) Risk reduction: Process mineralogy helps to identify possible processing problems, such as low metal recovery and high processing costs, by analyzing ore samples in detail. This information helps identify and mitigate risks at an early stage, leading to better risk control when using methods such as NPV and IRR. (3) Optimize project design: Understanding the detailed characteristics of ore can guide more efficient mine design and processing processes to maximize economic returns. This optimization directly affects the NPV and IRR of the project.[16]

In recent years, with the rapid development of technology, new methods of manganese ore beneficiation have appeared.[2] Although many scholars have done a lot of research on low-grade manganese ore in Chengkou, Chongqing, their research direction is mainly inclined to beneficiation test, and relatively little research on process mineralogy, and no technical and economic analysis has been made on it. In this paper, the process mineralogy of Chongqing Chengkou low-grade manganese ore will be studied in order to determine the mineral types and beneficiation methods of Chongqing Chengkou manganese ore. In addition, this study has carried out a technical and economic evaluation of the processing technology of Chengkou in Chongqing. Economic analysis was carried out through the internal return on investment (IRR), NPV, and the PBP. Sensitivity analysis was carried out on raw material cost, initial investment, main cost, and operating cost of manganese ore price change.[17] Technical and economic analysis was carried out based on three beneficiation methods: flotation, high-intensity magnetic separation, and gravity separation. Combining process mineralogy with NPV-, IRR-, and PBP-based investment evaluation methods can improve the quality of mining investment decisions and optimize the economic performance of projects while reducing environmental and social risks. It provides the theoretical basis for the development and utilization of manganese ore in the later stage and provides the process mineralogy support for the removal of impurities and beneficiation of manganese ore, so as to realize the efficient utilization of mineral resources.

## 2. EXPERIMENTAL METHOD

**2.1. Sample Preparation.** A batch of high-phosphorus manganese ore and high-sulfur manganese ore samples collected from Chengkou, Chongqing were analyzed. To obtain a tomography image of a multiphase filled particle bed for each sample, we prepared the sample in a 5 mm plastic cylindrical tube. The bottom of the plastic cylinder tube is first sealed with a plastic sheet or polystyrene foam, and then the particles are filled in the plastic cylinder tube to hold the particles in place and form a bed of filled particles. Finally, the



https://doi.org/10.1021/acsomega.3c10272
ACS Omega 2024, 9, 10929−10936

top of the plastic cylinder was sealed with the same material as the bottom of the tube. These particles are packed tightly together to ensure that no particles move during the scan so that a clear and blurry image can be obtained after the tomography scan.[3] The technical roadmap for the process mineralogy study of entire manganese is shown in Figure 1.

**2.2. Chromatographic Data Acquisition.** In this paper, the original samples of high-phosphorus manganese ore and high-sulfur manganese ore were analyzed. Data collection was performed by the HRXMT device (MicroXCT-400). A set of 994 projection slices, each consisting of a 992 × 1013 pixel array, was collected by rotating a plastic cylindrical tube (filled particle bed) between an X-ray source and a high-resolution detector and then reconstructed in 3D space with a voxel resolution of 4.59 $\mu$m. The basic principle of a high-resolution X-ray microtomography system is shown in Figure 2.[4]

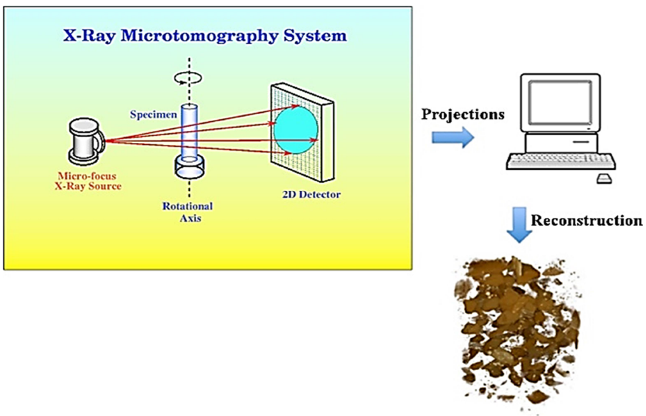


**Figure 2.** Data acquisition process.

**2.3. Analysis of Chemical Composition of Ore.** *2.3.1. Analysis Method.* Through a series of steps, such as image preprocessing, noise reduction, 3D images watershed segmentation of contact particles, and subsequent analysis of the original composition of the ore sample, the quantitative information on the sample image is obtained image segmentation is very important for our research because the 3D image Segmentation better preserves the distribution of minerals.[5] In order to investigate the grade and type of elements contained in the ore, we analyze the chemical composition of the ore and downstream products to determine the grade and grade of the main and minor components in the ore, laying the foundation for the mining of the ore. technology. Among them, X-ray diffraction analysis can obtain the original mineral phase composition and X-ray fluorescence spectroscopic analysis can obtain the original mineral element composition. This paper intends to combine two spectral analysis methods to analyze the chemical composition of high-phosphorus manganese ore and high-sulfur manganese ore.[6]

In the early image processing process, image segmentation is very important to our research. For the quantitative analysis of mineralogy, segmentation provides information about each grain in a packed grain bed, resulting in individual grain histograms to characterize the mineral phases associated with each grain. The detailed segmentation steps are as follows. First, the original 3D HRXMT images are preprocessed and denoised using a nonlocal averaging filter. Second, feature-based classification is applied to generate a binary image that separates the foreground (solid phase) from the background (air). The binary image is then subjected to the same processing as for watershed segmentation, such as distance transformation, marker definition, and finally flooding. Finally, a segmented image is obtained. Figure 3 shows the complete processing sequence for watershed segmentation.[7,8]

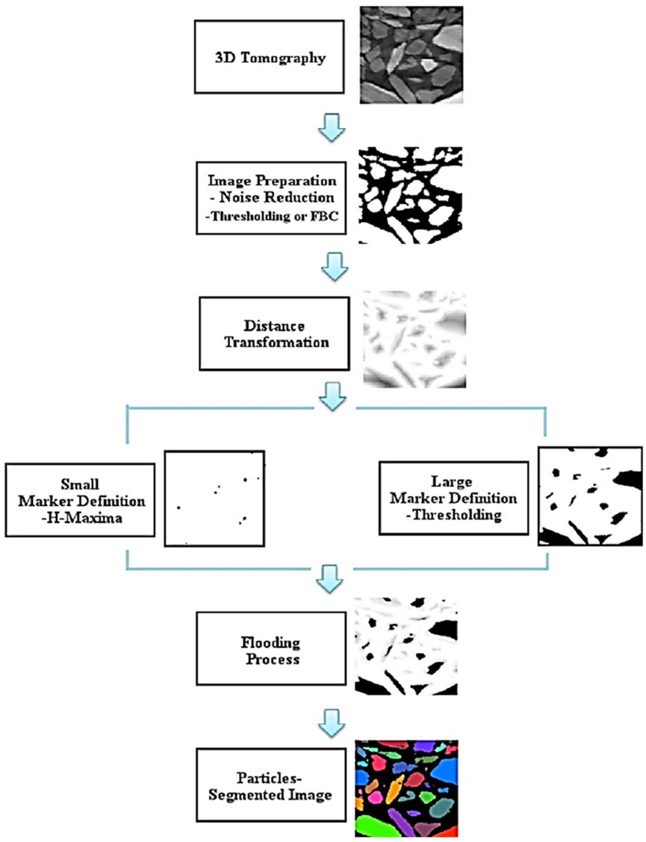


**Figure 3.** Watershed segmentation process.

*2.3.2. Noise Reduction.* Due to statistical differences, there is always noise in CT images when attenuation coefficient values are converted to CT numbers. The presence of noise in the image leads to difficulties in subsequent image processing steps. In general, a filtering process must be applied to the input image to minimize noise and improve image quality.[9] In this experiment, a nonlocal mean filter is used to denoise the original image.

*2.3.3. Separation of Particles from the Background.* After denoising the original image, particles are usually separated from the background. Threshold processing is used to segment particle phases from the background to generate a binary image.[10] The threshold is the value of the attenuation coefficient (CT number) that separates the background (air) from the foreground (mineral particles). Figure 4 shows an example of cross-sectional sections of 3D tomography data from a high-phosphorus manganese deposit. The histogram shows the total number of voxel numbers for the entire (992 × 1013 × 994) data set. Finally, a binary image with a threshold of 24 nm is obtained.

*2.3.4. Distance Transformation.* The key to the segmentation process is to determine the markings and locations of particles. Considering the irregularity of rock particle shape, distance transformation is used to assist the definition of the mark.[11] The range-varying image determines the distance of


https://doi.org/10.1021/acsomega.3c10272
ACS Omega 2024, 9, 10929−10936

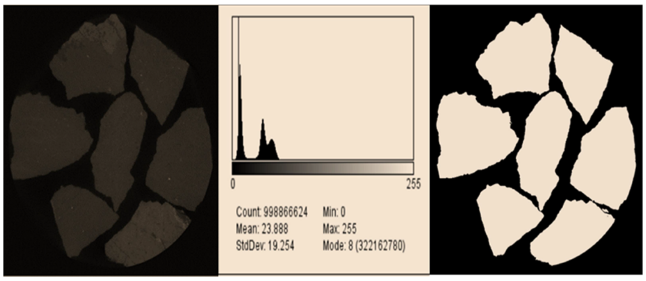


**Figure 4.** Separation of particles from background using traditional thresholds for high-phosphorus manganese ore. The reconstructed image (original image, left) was obtained by using high-speed X-ray tomography. The histogram showed a threshold of 24. The final binary segmentation image is shown on the right.

each pixel from the nearest background pixel. Figure 5 shows the particles of the manganese ore sample undergoing a distance change.

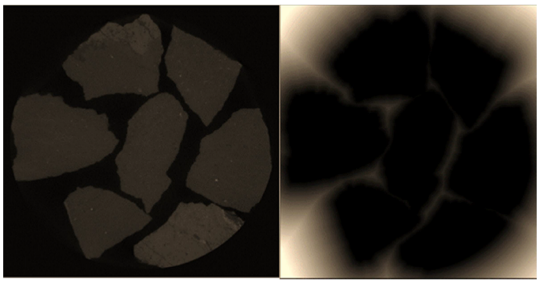

**Figure 5.** Example of distance transformation of high-phosphorus manganese ore. Two-dimensional slice view of 3D high-resolution X-ray tomography data (left). Distance transform image is shown in black and white (right).

*2.3.5. Tag Definition.* In many complex segmentation applications, the most important step is tag extraction. Mark unique regions of space to distinguish unique particles. The accuracy of the mark definition will directly determine the quality of segmentation. In order to achieve multiscale image segmentation, first, the marks of larger particles are directly obtained by threshold processing of the images after distance transformation. The marks of the smaller particles are then formed by subtracting the marks of the larger particles from the original image. Finally, the tags of the larger and smaller particles are combined to obtain all of the tags.

*2.3.6. Watershed Segmentation.* Once the tag is defined, each particle can be assigned an identification number.[12] Then, watershed transform and flood processing are used to segment the particle image. Figure 6 shows the segmented 3D image.

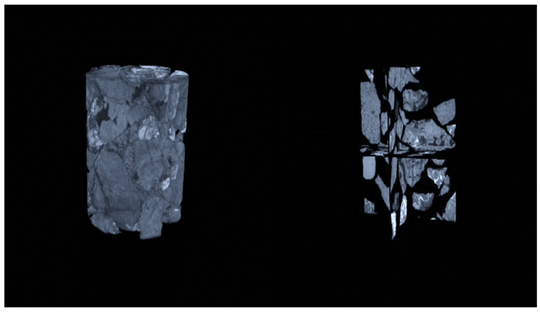

**Figure 6.** 3D segmentation of high-phosphorus manganese ore.

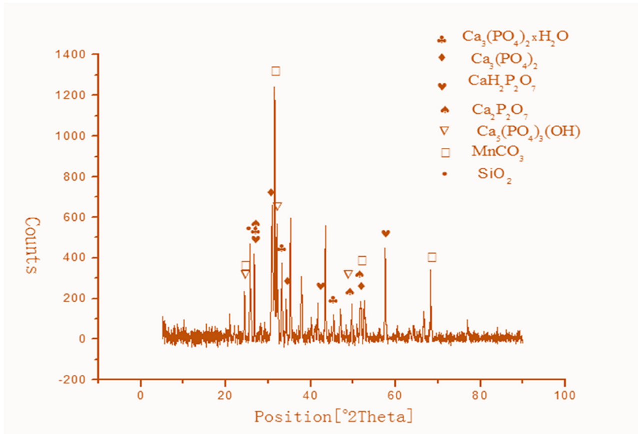


**Figure 7.** X-ray diffraction pattern of phosphorus-rich manganese ore.

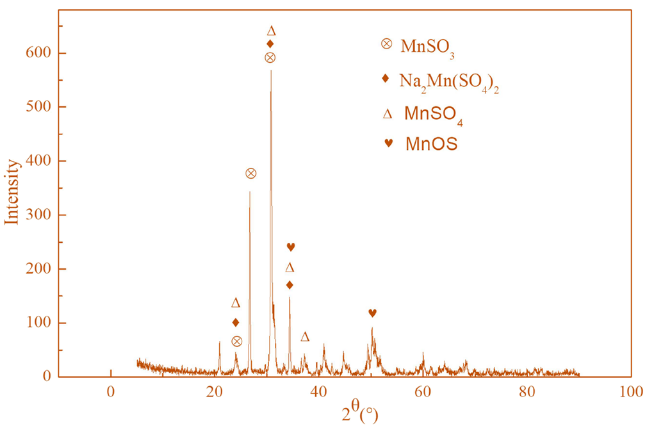


**Figure 8.** High-sulfur manganese ore of XRD picture.

## 3. RESULTS AND DISCUSSION

**3.1. XRD and XRF Analysis Results of Two Groups of Original Samples.** The results of XRD analysis of the original samples of the two groups are shown in Figures 7 and 8, and the results of XRF analysis of the original samples are shown in Tables 1 and 2.

As can be seen from Figure 7 and Table 1, the original composition of the high-phosphorus manganese ore contains silicate, apatite ($Ca_5(PO_4)_3(OH)$), rhodochromite ($MnCO_3$), calcite, quartz ($SiO_2$), and other phosphorus-rich minerals, and the manganese element mainly exists in the form of carbonate manganese salt. In addition, the grade of manganese extracted from the ore is 28.829%, Mn/Fe = 13.534, and P/Mn = 0.039 (P/Mn greater than 0.006 is high phosphorus), which belongs to high-phosphorus poor iron-rich manganese ore. In order to achieve the purpose of enriching manganese minerals, the components that need to be excluded are mainly $SiO_2$ and CaO, followed by MgO, $Al_2O_3$, $K_2O$ and P, S, and other harmful elements.

It can be seen from Figure 8 and Table 2 that the original composition of the high-sulfur manganese ore contains silicate, rhodochrozite, calcite, pyrite ($FeS_2$), etc., and the main form of manganese is sulfur-containing manganese salt. In addition, the grade of manganese extracted from the ore is 22.40%, Mn/Fe = 34.46, S/Mn = 0.180, belonging to high-sulfur iron and manganese poor ore. In order to achieve the purpose of enriching manganese minerals, the components that need to be


https://doi.org/10.1021/acsomega.3c10272
ACS Omega 2024, 9, 10929−10936

Table 1. XRF Analysis of the Element in Phosphorus-Rich Manganese Ore

| element | O | Mn | Si | Mg | Ca | Al | Fe | K | Na | S |
|---|---|---|---|---|---|---|---|---|---|---|
| content % | 39.260 | 28.829 | 10.316 | 2.8281 | 9.522 | 2.13 | 2.13 | 0.97 | | 2.09 |
| element | P | Ti | V | Sr | Ba | Zn | Co | Cr | Rb | Ni |
| content % | 1.11 | 0.217 | | 0.035 | 0.11 | 0.06 | | | | 0.08 |

Table 2. Analysis of Multielements of the High-Sulfur Manganese Ore

| element | O | Mn | Si | Mg | Ca | Al | Fe | K | Na | S |
|---|---|---|---|---|---|---|---|---|---|---|
| content % | 39.27 | 22.40 | 12.86 | 4.65 | 12.89 | 1.66 | 0.65 | 0.34 | 0.18 | 4.04 |
| element | P | Ti | V | Sr | Ba | Zn | Co | Cr | Rb | Ni |
| content % | 0.28 | 0.048 | | 0.024 | | 0.015 | | 0.014 | | 0.018 |

excluded are mainly $SiO_2$ and CaO, followed by MgO, $Al_2O_3$, $K_2O$ and P, S and other harmful elements.

Based on the above analysis of the two groups of manganese ore samples from Chengkou, Chongqing, it can be divided into carbonate-type manganese ore and oxidizing manganese ore. Among them, carbonate manganese ore should be the main ore process type in the study area. Oxidized manganese ore is usually distributed on the surface of the ore body and has been exploited in large quantities. It is not the main ore process type studied at present.

**3.2. Mineral Composition and Distribution Characteristics of Main Minerals are Discussed.** It is of great significance to study the mineral composition and distribution characteristics of the ore. In minerals, the same element usually has different forms of existence, and the same element may also form a similar substance that makes the properties of each other greatly different, so the selection of mineral processing methods and mineral processing processes is not the same. Therefore, it is of great significance to study mineral composition and distribution characteristics for determining the mineral processing method and mineral processing process.

X-ray diffraction analysis can use the X-ray diffraction data to phase analyze the mineral phases existing in the sample to be tested,[13] while X-ray three-dimensional tomography analysis can use the tomography data to quantitatively analyze the information on each particle in the sample to be tested, so as to generate a single particle histogram to characterize the mineral phase belonging to each particle, and then reconstruct a three-dimensional map with mineral distribution.

Through two kinds of analysis of the two groups of raw ore samples from Chengkou, Chongqing, we can see that the raw ore mainly consists of carbonate, silicate, and oxide, in addition to a small amount of sulfide and a small amount of clay minerals. The carbonate minerals are mainly rhodochrogite and a small amount of calcite. Quartz is the main oxide mineral; silicate minerals are mainly silicate; and sulfide is mainly pyrite. The mineral types and percentage contents of various minerals in the original samples of the two groups are, respectively, shown in Tables 3 and 4; X-ray diffraction analysis diagrams are, respectively, shown in Figures 7 and 8; distribution characteristics of major minerals are, respectively, shown in Figures 9 and 10.

Table 3. Composition and Content of Minerals in the Original Samples of High-Phosphorus Manganese Ore

| mineral name | silicate | rhodochroite | apatite | calcite | other |
|---|---|---|---|---|---|
| percentage content | 43.8% | 23.9% | 12.3% | 12.1% | 7.9% |

Table 4. Composition and Content of Minerals in the Original Samples of High-Sulfur Manganese Ore

| mineral name | silicate | rhodochroite | calcite | pyrite |
|---|---|---|---|---|
| percentage content | 15.8% | 10.9% | 71.5% | 1.8% |

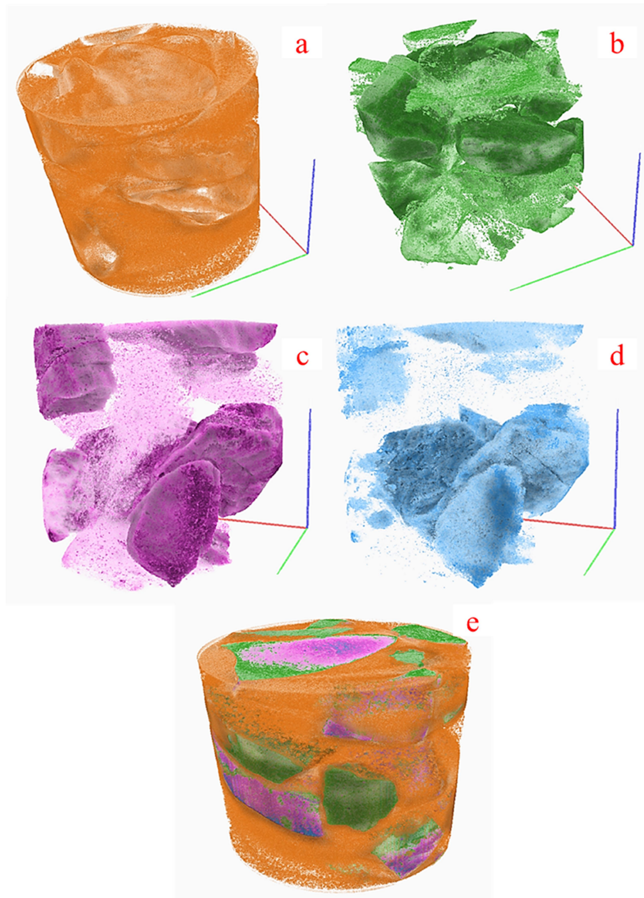


Figure 9. Distribution pattern of silicate minerals (a), rhodochromite (b), apatite (c), and calcite (d) in the original samples of high-phosphorus manganese ores (e).

The phosphorus content of manganese ore in China is relatively high, P/Mn is about 0.01 on average, and the metallurgical manganese ore requires P/Mn < 0.003, so the manganese ore in China is a typical high-phosphorus manganese ore. In the investigated manganese deposits, about 50% of the phosphorus content exceeds the standard, and only 6% meets the standard of high-quality manganese ore. Phosphorus in manganese ore mainly exists in the form of


https://doi.org/10.1021/acsomega.3c10272
ACS Omega 2024, 9, 10929−10936

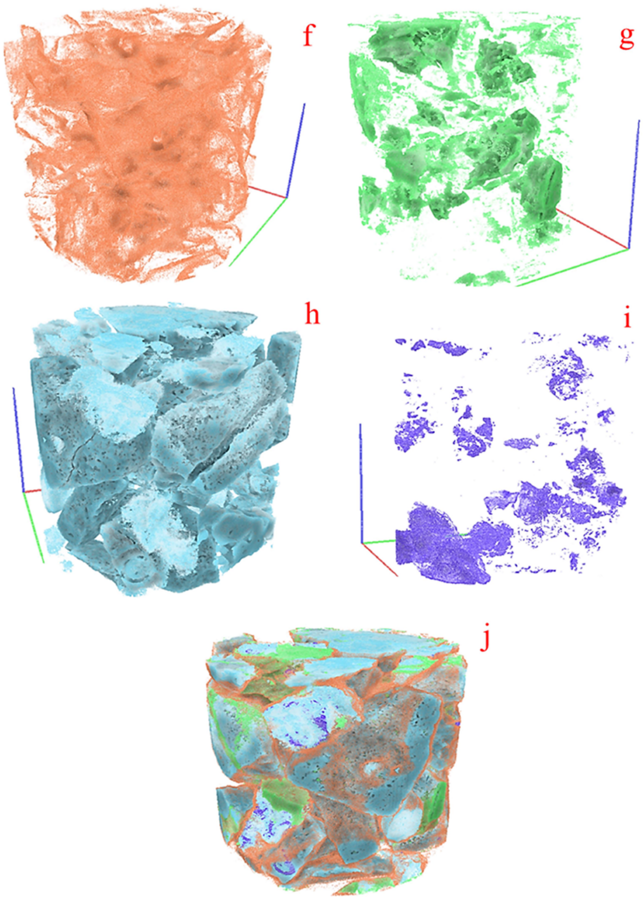


**Figure 10.** Distribution patterns of silicate minerals (f), rhodochromite (g), calcite (h), and pyrite (i) in the original samples of high-sulfur manganese ores (j).

apatite. It is difficult to achieve monomer dissociation because of the fine particle size of phosphate-containing minerals or their homogeneity with manganese minerals. At present, most of the separation methods of manganese ore in the world use flotation, strong magnetic separation, and gravity separation, and manganese oxide ore and carbonate manganese ore contain some difficult ore, manganese and iron, phosphorus or gangue close symbiosis, disseminated particle size is very fine, difficult to separate, you can consider the use of manganese-rich slag smelting method, in addition to roasting, microbial leaching, and other methods. Manganese ores in Chongqing Chengkou are often produced in aggregate form, but often with iron, phosphorus, and gangue symbiosis, the particle size is finer, difficult to separate, and gravity separation is only suitable for simple structure, coarse grain size of manganese ores, so the gravity separation method for Chongqing Chengkou manganese ore sorting effect is not good.

The target mineral of the Chongqing Chengkou manganese ore sample is carbonate manganese ore (rhombic manganese ore), the content of which is up to 82.9% in manganese minerals, and a small amount of silicate manganese minerals should be based on the properties of carbonate manganese ore in the selection of the mineral separation method. Because carbonate manganese minerals and silicate manganese minerals are weak magnetic minerals and because the specific magnetization coefficient of these two types of manganese minerals and gangue minerals and minerals containing harmful impurities is a relatively large difference, strong magnetic separation is one of the most suitable means for the separation of this mine. The specific magnetization coefficient and specific gravity of common manganese minerals and gangue minerals are shown in Table 5.

**Table 5. Specific Magnetic Susceptibility and Specific Gravity of Common Manganese Minerals and Gangue Minerals**

| mineral | specific magnetization factor (K) | specific gravity |
|---|---|---|
| rhodochrosite | 1.3−1.7 | 3.6−3.7 |
| brown manganese ore | 1.5 | 4.72−4.83 |
| pyrolusite | 0.34 | 4.7−5.0 |
| manganite | 1.01 | 4.2−4.33 |
| psilomelane | 0.3−0.6 | 4.7 |
| manganese calcite | 0.83−1.2 | 2.9 |
| dolomite | 0.34 | 2.85 |
| quartz | 0.003−0.13 | 2.65 |
| apatite | 0.05 | 3.18−3.21 |

**3.3. Technical and Economic Evaluation.** In order to analyze the economic indexes of flotation, high-intensity magnetic separation, and gravity separation in the processing of Chongqing Chengkou manganese ore, the beneficiation methods were evaluated. Using NPV, IRR, and PBP as economic indicators, the economic feasibility of each mineral processing method was evaluated.[15] We listed specific data for each technology and calculated their NPV, IRR, and PBP. The calculated data and Table 6 are shown below.

**Table 6. Comparison of Economic Indexes of Flotation, High-Intensity Magnetic Separation, and Gravity Separation Methods**

| beneficiation method | flotation | high-intensity magnetic separation | gravity separation |
|---|---|---|---|
| annual production (tons) | 10,000 | 10,000 | 10,000 |
| manganese content (%) | 30% | 30% | 30% |
| manganese ore price (per ton) | 100 | 100 | 100 |
| mining cost (million) | 10 | 10 | 10 |
| shipping cost (million) | 5 | 5 | 5 |
| processing cost (million) | 3 | 4 | 2 |
| equipment maintenance cost (million) | 2 | 2 | 2 |
| manpower cost (million) | 1.5 | 1.5 | 1.5 |
| environmental cost (million) | 0.5 | 0.5 | 0.5 |
| investment discount rate | 10% | 10% | 10% |
| net present value (NPV) (million) | 11.75 | 7.24 | 10.47 |
| internal rate of return (IRR) | 14.09% | 11.34% | 15.73% |
| payback period (PBP) (years) | 3 | 4 | 3 |

Flotation separation technology of manganese ore:

NPV = $\Sigma[(\text{annual income} - \text{annual expenditure})/(1 + 0.10)^t] - 70$ million ≈ 11,753,975

IRR ≈ 14.09%

PBP ≈ 3 years

High-intensity magnetic separation technology:

NPV = $\Sigma\ [(\text{annual income} - \text{annual expenditure})/(1 + 0.10)^t] - 87.5$ million ≈ 7,244,778

IRR ≈ 11.34%


https://doi.org/10.1021/acsomega.3c10272
ACS Omega 2024, 9, 10929−10936

PBP ≈ 4 years

Gravity separation of manganese ore technology:

NPV = Σ [(annual income − annual expenditure)/(1 + 0.10)$^t$] − 54 million ≈ 10,469,907

IRR ≈ 15.73%

PBP ≈ 3 years

According to the technical requirements of modern industrial development, modern industrial development should follow the principle of high resource utilization and low environmental pollution. On the basis of efficient dephosphorization, special attention should be paid to the recovery of manganese to reduce the energy loss in the process. As far as possible, no environmental pollution is caused in the process to realize the harmless process.[14] The dephosphorization technology of high-intensity magnetic separation is more in line with the requirements of modern technology. From a technical and economic point of view, flotation technology has the highest NPV of 11,753,975, followed by gravity separation technology (10,469,907), and high-intensity magnetic separation technology has the lowest NPV of 7,244,778. From the IRR point of view, the IRR of reseparation is the highest (15.73%), followed by flotation (14.09%), and the IRR of high-intensity magnetic separation is the lowest (11.34%). In terms of the investment PBP, the investment PBP of manganese ore technology flotation and gravity separation is 3 years, while the investment PBP of manganese ore strong magnetic separation technology is 4 years. In summary, high-intensity magnetic separation is the best solution for the processing method of Chongqing Chengkou manganese ore, but the flotation separation technology has the highest NPV and IRR and the investment PBP is short.

## 4. CONCLUSIONS

The mineral technology of Chengkou manganese ore in Chongqing is studied in this paper. The results show that high-intensity magnetic separation is the most suitable technology for the Chengkou manganese mine in Chongqing. However, the analysis of economic indicators, such as flotation, high-intensity magnetic separation, and gravity separation through the IRR, NPV, and PBP, shows that flotation separation technology is the best choice because it has the highest NPV and IRR and the short PBP. This study combines process mineralogy research with technical and economic analysis to improve the quality of mining investment decisions and optimize the economic performance of projects, while reducing environmental and social risks. It provides the theoretical basis for the development and utilization of manganese ore in the later stage, provides the process mineralogy support for the separation of manganese ore, and provides a reference for other mining companies to choose the most suitable beneficiation method according to their specific ore species, so as to realize the efficient utilization of mineral resources.

## ■ AUTHOR INFORMATION

### Corresponding Author

**Facheng Qiu** − *School of Chemistry and Chemical Engineering, Chongqing University of Technology, Chongqing 400054, China;* orcid.org/0000-0002-9998-9175; Email: qiufachengandl@126.com

### Authors

**Wensheng Li** − *School of Chemistry and Chemical Engineering, Chongqing University of Technology, Chongqing 400054, China*

**Guangchao Jiang** − *School of Chemistry and Chemical Engineering, Chongqing University of Technology, Chongqing 400054, China*

**Guangzhou Yang** − *School of Chemistry and Chemical Engineering, Chongqing University of Technology, Chongqing 400054, China*

Complete contact information is available at: https://pubs.acs.org/10.1021/acsomega.3c10272

### Notes

The authors declare no competing financial interest.

## ■ ACKNOWLEDGMENTS

This research was supported by the Science and Technology Research Program of Chongqing Education Commission (KJQN202001112), Chongqing Natural Science Foundation (cstc2021jcyj-msxmX0184), and Chongqing Natural Science Foundation Venture Development Joint Fund (CSTB2023NSCQ-LZX0095).

## ■ REFERENCES

(1) Zhang, C.; Yang, S.; Zhang, X.; Xia, Y.; Li, J. Extended Line Defect Graphene Modified by the Adsorption of Mn Atoms and Its Properties of Adsorbing CH4. *Nanomaterials* **2022**, *12* (4), 697.

(2) Kujala, K.; Besold, J.; Mikkonen, A.; Tiirola, M.; Planer-Friedrich, B. Abundant and Diverse Arsenic-Metabolizing Microorganisms in Peatlands Treating Arsenic-Contaminated Mining Wastewaters. *Environmental Microbiology* **2020**, *22* (4), 1572−1587.

(3) Wang, Y.; Lin, C. L.; Miller, J. D. Quantitative Analysis of Exposed Grain Surface Area for Multiphase Particles Using X-Ray Microtomography. *Powder Technol.* **2017**, *308*, 368−377.

(4) Wang, Y.; Lin, C. L.; Miller, J. D. Improved 3D Image Segmentation for X-Ray Tomographic Analysis of Packed Particle Beds. *Minerals Engineering* **2015**, *83*, 185−191.

(5) Wang, Y.; Lin, C. L.; Miller, J. D. 3D Image Segmentation for Analysis of Multisize Particles in a Packed Particle Bed. *Powder Technol.* **2016**, *301*, 160−168.

(6) Lin, C. L.; Miller, J. D. 3D Characterization and Analysis of Particle Shape Using X-Ray Microtomography (XMT). *Powder Technol.* **2005**, *154* (1), 61−69.

(7) Puvvada, S.; Lin, C. L.; Miller, J. D. High Speed X-Ray Computed Tomography for Plant-Site Analysis of Pebble Phosphate. *Minerals Engineering* **2019**, *130*, 129−141.

(8) Videla, A. R.; Lin, C. L.; Miller, J. D. 3D Characterization of Individual Multiphase Particles in Packed Particle Beds by X-Ray Microtomography (XMT). *Int. J. Miner. Process.* **2007**, *84* (1), 321−326.

(9) Alhussaini, A. J.; Steele, J. D.; Nabi, G. Comparative Analysis for the Distinction of Chromophobe Renal Cell Carcinoma from Renal Oncocytoma in Computed Tomography Imaging Using Machine Learning Radiomics Analysis. *Cancers* **2022**, *14* (15), 3609.

(10) Jiang, L.; Cheng, Y.; Gao, S.; Zhong, Y.; Ma, C.; Wang, T.; Zhu, Y. Emergence of Social Cluster by Collective Pairwise Encounters in Drosophila. *eLife* **2020**, *9*, No. e51921.

(11) Nesterov, S.; Chesnokov, Y.; Kamyshinsky, R.; Panteleeva, A.; Lyamzaev, K.; Vasilov, R.; Yaguzhinsky, L. Ordered Clusters of the Complete Oxidative Phosphorylation System in Cardiac Mitochondria. *International Journal of Molecular Sciences* **2021**, *22* (3), 1462.

(12) Rensen, E.; Mueller, F.; Scoca, V.; Parmar, J. J.; Souque, P.; Zimmer, C.; Di Nunzio, F. Clustering and Reverse Transcription of HIV-1 Genomes in Nuclear Niches of Macrophages. *EMBO Journal* **2021**, *40* (1), No. e105247.

(13) Ahmed, S. S.; Schattgen, S. A.; Frakes, A. E.; Sikoglu, E. M.; Su, Q.; Li, J.; Hampton, T. G.; Denninger, A. R.; Kirschner, D. A.; Kaspar, B.; Matalon, R.; Gao, G. rAAV Gene Therapy in a Canavan's Disease Mouse Model Reveals Immune Impairments and an Extended Pathology Beyond the Central Nervous System. *Molecular Therapy* **2016**, *24* (6), 1030−1041.

(14) Tang, M.; Wang, X.; Niu, W.; Fu, J.; Zhu, M. How Financial Development Scale and R&D Influence Regional Innovation Efficiency: Empirical Evidence from the Financial Industry. *Environ. Sci. Pollut Res.* **2023**, *30* (22), 61257−61270.

(15) Werner, K.; Risko, N.; Burkholder, T.; Munge, K.; Wallis, L.; Reynolds, T. Cost−Effectiveness of Emergency Care Interventions in Low and Middle-Income Countries: A Systematic Review. *Bull. World Health Organ* **2020**, *98* (5), 341−352.

(16) Gwak, I.-S.; Hwang, J.-H.; Lee, S.H. Techno-economic Evaluation of an Ethanol Production Process for Biomass Waste. *Appl. Chem. Eng.* **2016**, *27* (2), 171−178.

(17) Zhang, C.; Jun, K.-W.; Gao, R.; Lee, Y.-J.; Kang, S. C. Efficient utilization of carbon dioxide in gas-to-liquids process: Process simulation and techno-economic analysis. *Fuel* **2015**, *157*, 285−291.



https://doi.org/10.1021/acsomega.3c10272
*ACS Omega* 2024, 9, 10929−10936